HHS Public Access

Author manuscript

Pflugers Arch. Author manuscript; available in PMC 2016 January 06.

Published in final edited form as:

Pflugers Arch. 2016 January ; 468(1): 131–142. doi:10.1007/s00424-015-1717-1.

Functional response of the isolated, perfused normoxic heart to pyruvate dehydrogenase activation by dichloroacetate and pyruvate

Rafael Jaimes 3rd[1], **Sarah Kuzmiak-Glancy**[1], **Daina M. Brooks**[1], **Luther M. Swift**[2], **Nikki G. Posnack**[2], and **Matthew W. Kay**[1,2]

[1]Department of Biomedical Engineering, The George Washington University, GWU Science and Engineering Hall, 800 22nd Street NW, Suite 5000, Washington, DC 20052, USA

[2]Department of Pharmacology and Physiology, The George Washington University, Washington, DC 20052, USA

Abstract

Dichloroacetate (DCA) and pyruvate activate pyruvate dehydrogenase (PDH), a key enzyme that modulates glucose oxidation and mitochondrial NADH production. Both compounds improve recovery after ischemia in isolated hearts. However, the action of DCA and pyruvate in normoxic myocardium is incompletely understood. We measured the effect of DCA and pyruvate on contraction, mitochondrial redox state, and intracellular calcium cycling in isolated rat hearts during normoxic perfusion. Normalized epicardial NADH fluorescence (nNADH) and left ventricular developed pressure (LVDP) were measured before and after administering DCA (5 mM) or pyruvate (5 mM). Optical mapping of Rhod-2AM was used to measure cytosolic calcium kinetics. DCA maximally activated PDH, increasing the ratio of active to total PDH from 0.48±0.03 to 1.03 ±0.03. Pyruvate sub-maximally activated PDH to a ratio of 0.75±0.02. DCA and pyruvate increased LVDP. When glucose was the only exogenous fuel, pyruvate increased nNADH by 21.4±2.9 % while DCA reduced nNADH by 21.4±6.1 % and elevated the incidence of premature ventricular contractions (PVCs). When lactate, pyruvate, and glucose were provided together as exogenous fuels, nNADH increased with DCA, indicating that PDH activation with glucose as the only exogenous fuel depletes PDH substrate. Calcium transient time-to-peak was shortened by DCA and pyruvate and SR calcium re-uptake was 30 % longer. DCA and pyruvate increased SR calcium load in myocyte monolayers. Overall, during normoxia when glucose is the only exogenous fuel, DCA elevates SR calcium, increases LVDP and contractility, and diminishes mitochondrial NADH. Administering DCA with plasma levels of lactate and pyruvate mitigates the drop in mitochondrial NADH and prevents PVCs.

Matthew W. Kay, phymwk@gwu.edu.

Compliance with ethical standards All applicable international, national, and institutional guidelines for the care and use of animals were followed. All procedures performed in studies involving animals were in accordance with the ethical standards of the George Washington University.

The authors declare that they have no conflict of interest.

Keywords

Pyruvate dehydrogenase; Dichloroacetate; NADH; Cardiac

Introduction

Dichloroacetate (DCA) improves the recovery of function during post-ischemic reperfusion in isolated heart preparations [28, 30, 36, 37, 45]. The general mechanism is thought to be the activation of pyruvate dehydrogenase (PDH) via the inhibition of PDH kinase (PDHK) by DCA. This promotes full glucose oxidation by increasing flux through PDH, which is primarily in its phosphorylated, inactive form during the first few minutes of reperfusion [23, 27, 39]. The conversion of pyruvate to acetyl-CoA by the pyruvate dehydrogenase complex is a key regulatory step, especially when glycolytic activity is high, as it is during ischemia [6]. Because of this, the activation level of PDH is an important modulator of both substrate utilization and cardiac function.

Improved function upon reperfusion with DCA is attributed to the correction of the imbalance between glycolysis and full glucose oxidation after ischemia [32, 36]. However, pyruvate, which also activates PDH, improves post-ischemic function as well [18, 34]. Administering pyruvate would not correct an imbalance between glycolysis and full glucose oxidation: in fact, any imbalance would be exacerbated. Numerous other studies have investigated the mechanisms by which pyruvate improves cardiac function without the confounding variable of ischemia [10, 46, 52]; however, there are very few investigations of the mechanisms of DCA in the absence of ischemia.

Increased pyruvate levels improve contractile performance during normoxia [10, 35]. Increased inotropy after administering exogenous pyruvate is due to increased TCA flux that increases mitochondrial NADH [43]. Cytosolic phosphorylation potential ([ATP]/[ADP][P_i]) is also elevated, as demonstrated in isolated perfused hearts [10, 22], as well as in vivo [25]. Higher [ATP]/[ADP][P_i] improves the efficiency of ATP-dependent processes such as sarco/endoplasmic reticulum Ca^{2+}-ATPase (SERCA) [11] and the actin-myosin ATPase. Abundant pyruvate also stabilizes the ryanodine receptor (RyR) to reduce sarcoplasmic (SR) Ca^{2+} leak [11, 52]. The overall effect is greater SR Ca^{2+} load and release, increased force production, and increased availability of high-energy phosphates for contraction, all of which occur without a change in heart rate [35].

The understanding of DCA mechanisms is incomplete without additional insight into how DCA might modulate function during normoxia. Indeed, administering DCA to cardiac tissue, whether normoxic or not, should shift substrate preference from endogenous fatty acids to carbohydrates. While fatty acids are the preferred substrate in normoxia [29], DCA administration causes fatty acid oxidation to drop to almost zero while glucose and pyruvate oxidation increase significantly, regardless of the presence of exogenous fat supply [31]. Improved understanding of this effect of DCA in the normoxic perfused heart, and a comparison to the effect of administering exogenous pyruvate, could provide additional insight into the functional response of cardiac tissue to DCA.

Our objective was to study the effects of DCA on PDH activation, downstream mitochondrial NADH production and consumption, calcium handling, myocardial contractile function, and the potential for causing arrhythmias in the normoxic perfused heart. Our approach was to compare the effects of activating PDH with either DCA or exogenous pyruvate. We hypothesized that administration of 5 mM pyruvate, with 6 mM glucose provided as fuel, would increase steady-state NADH and LVDP. We hypothesized the administration of DCA, with 6 mM glucose provided as the fuel, would cause an initial increase in NADH concentration as PDH flux increased; however, this would be followed by a decrease in NADH due to an eventual PDH substrate limitation resulting from high PDH flux and increased demand for NADH secondary to increased LVDP. Furthermore, we predict DCA may increase the incidence of premature ventricular contractions due to reduced endogenous pyruvate concentration, which may blunt the stabilizing effects of pyruvate on RyR [52]. We hypothesize that pyruvate depletion with DCA and downstream effects can be prevented with physiologic plasma concentrations of lactate (1 mM) and pyruvate (0.2 mM) [47]. While both 5 mM DCA and pyruvate are expected to increase LVDP, they are also expected to affect calcium handling similarly, specifically by enhancing SR calcium load.

Materials and methods

Heart preparation

The George Washington University's Animal Care and Use Committee approved all animal protocols. Sprague–Dawley rats (male, 300–350 g) were anesthetized with an intraperitoneal injection of Telazol (40 mg/kg). Upon cessation of pain reflexes, the heart was exposed via thoracotomy and rapidly bathed in cold Krebs-Henseleit solution (KH) to slow heart rate. Hearts were then excised and rinsed in a bath of ice-cold KH. The aorta was rapidly cannulated then flushed with 500 units of heparin mixed with KH perfusate that contained (in mM): 118 NaCl, 4.7 KCl, 1.25 $CaCl_2$, 0.57 $MgSO_4$, 1.17 KH_2PO_4, 25 $NaHCO_3$, 6 glucose, and 500 mU/L insulin. Exogenous fatty acids were not added to the perfusate for the following reasons: (1) there is evidence that isolated perfused hearts have ample endogenous fat to maintain normal contractile function for at least 60 min [38]; (2) DCA administration causes fatty acid oxidation to drop to approximately 0, regardless of the presence of exogenous fatty acids [31]; (3) our objective was to control exogenous substrates utilization to systematically compare the functional response of DCA and exogenous pyruvate.

Hearts were then transferred to a constant pressure (70 mmHg, 37±1 ° C) perfusion system that was designed to provide for controlled transition between baseline (control) perfusate and perfusate containing either 5 mM of pyruvate or DCA. This prevented the heart from being exposed to high concentrations that may result from bolus administration of pyruvate or DCA. Two separate reservoirs and pumps provided constant circulation and heating of each perfusate solution and a valve at the aortic cannula allowed for immediate switching between perfusates.

General protocol

The initial perfusate (baseline) was the KH solution described above. Hearts were closely monitored for electromechanical stability and signs of regional ischemia before beginning each protocol. Hearts that appeared to be damaged were excluded. After a baseline period of 10 min, the perfusate was switched to baseline KH perfusate containing one of three solutions: (a) 5 mM Na-Pyruvate (Pyr), (b) 5 mM Na-DCA (DCA), (c) baseline KH (control, Ctrl). 5 mM DCA is at the upper-end of reported DCA concentrations that are used in reperfusion studies [50]. The pyruvate concentration was chosen to match the DCA concentration (5 mM), although higher concentrations have been used in previous studies [46]. After the perfusate switch, left-ventricular developed pressure (LVDP), heart rate, and epicardial NADH fluorescence were recorded for an additional 40 min (see below), after which each heart was subjected to no-flow ischemia to record maximum NADH fluorescence.

A separate set of experiments was completed to study the effects of administering DCA to hearts perfused with physiologic levels of lactate and pyruvate (DCA-LP). In those studies DCA (5 mM) was administered to hearts perfused with baseline perfusate that also contained lactate (1 mM) and pyruvate (0.2 mM). The results of those studies were compared with the results of administering DCA to hearts perfused with only 6 mM glucose.

Left-ventricular developed pressure measurements and NADH imaging

Isovolumic LVDP was measured by inserting a latex balloon (size 5) into the LV using established techniques [17, 41]. The balloon was attached to a pressure transducer and the diastolic LV pressure was set to 10 mmHg using a spindle syringe. Pressure was continuously recorded using a bridge amplifier (World Precision Instruments) attached to a PowerLab data acquisition unit with LabChart software (ADInstruments). After each study, LVDP signals were differentiated and inotropy (max dP/dt) and lusitropy (min dP/dt) were analyzed at predetermined timepoints.

Epicardial NADH fluorescence (fNADH) was imaged as previously described [2, 49]. A UV LED spotlight (Mightex Systems) with a peak wavelength of 365 nm illuminated the anterior epicardial surface. Power output was set to 2 mW with a power density of approximately 0.16 mW/cm^2. At this light intensity, we did not observe significant fNADH photobleaching over the course of two hours (data not shown). Light emitted from the epicardial surface passed through a lens (Navitar, Inc), was band pass filtered at 475±25 nm (Chroma Technology), and imaged at two frames per second using a CCD camera (Andor iXon DV860). The anterior surface filled most of the imaging region; the majority of the image contained the LV. Epicardial fNADH was assumed to be primarily of mitochondrial origin because the fluorescence of mitochondrial NADH is dramatically enhanced by the binding of NADH to Complex I [7].

Average normalized fNADH signals were computed from fNADH images by manually selecting a large region of interest (ROI) that contained most of the visible epicardial surface. For each image, fNADH was averaged for all pixels in the ROI to provide a

temporal fNADH signal: fNADH(t). That signal was then normalized to compute nNADH(t) using the equation:

$$nNADH\,(t) = \frac{fNADH\,(t) - fNADH\,(t_{\text{baseline}})}{fNADH\,(t_{\text{ischemia}}) - fNADH\,(t_{\text{baseline}})} \quad (1)$$

where fNADH($t_{baseline}$) is the average fluorescence intensity during the initial 10 min baseline period and fNADH($t_{Ischemia}$) is the fluorescence intensity after global ischemia, which fully reduces NADH. This normalization sets fluorescence for global ischemia at 100 % and baseline fluorescence at 0 %. nNADH(t) was then used to compare changes in mitochondrial NADH concentration between hearts.

Measurement of PDH activation ratio

PDH activation was measured for hearts perfused with 6 mM glucose (Ctrl), 6 mM glucose +5 mM DCA (DCA), 6 mM glucose+5 mM pyruvate (Pyr), and 6 mM glucose+1 mM lactate+0.2 mM pyruvate+5 mM DCA (DCA-LP). PDH activity was determined as previously described by Gohil and Jones [15]. Ventricular tissue was homogenized (12.5 *%w/v*) and spun at 16,000×*g* for 5 s. The supernatant was then spun again for 5 min at 16,000×*g*. To measure PDH activity (PDHa), 0.5–0.7 mg protein was suspended in 50 μL of 100 mM P_i+2 % Triton solution, then placed in a 1-mL cuvette with (in millimolar): 50 Tris (pH=8.0), 2 $MgCl_2$, 2 pyruvate, 2 NAD, 2 TPP, and 0.2 KCN. Background was measured at 340 nm using a spectrophotometer (Molecular Devices). The addition of 20 mM CoA to the cuvette stimulated NADH production, which was measured for 2 min. Maximal, or total, PDH activity (PDHt) was measured by increasing the pyruvate and $MgCl_2$ concentrations to 20 mM. The ratio of baseline PDH activity to total PDH activity (PDHa:PDHt) determined the percent of total PDH that was active. Protein concentration was measured using a Pierce™ BCA protein assay kit (Life Technologies).

Cytosolic calcium imaging

Cytosolic Ca^{2+} transients were measured before and after administering DCA or pyruvate. Hearts were excised and Langendorff perfused as described above. The Ca^{2+} sensitive dye, Rhod-2AM (50 μg dissolved in 50 μL DMSO and mixed with 50 μL of 20 % Pluronic F-127), was mixed with 1 mL of 37 °C perfusate and injected into the bubble trap directly above the heart. Blebbistatin, an actin-myosin ATPase inhibitor, was added to both perfusate reservoirs (4.75 μM) to prevent motion artifact while imaging Rhod-2AM fluorescence [14]. Rhod-2AM was excited using an LED spotlight (output power at 2 mW) with a peak wavelength of 530 nm (Mightex Systems) and a 545±20-nm excitation filter (Chroma Technology). Emitted light passed through a lens (Navitar, Inc), was band pass filtered at 605±35 nm (Chroma Technology), and imaged at >600 frames per second using a CCD camera (Andor iXon DV860).

Hearts were monitored for 10 min with baseline KH after administration of blebbistatin and Rhod-2AM. Perfusate was then switched to a solution that was either baseline KH (Ctrl) or contained 5 mM pyruvate (Pyr) or 5 mM DCA (DCA). Ca^{2+} transients were imaged (2-s duration) at 2-min intervals during baseline perfusion and after the perfusate switch. When

imaging, hearts were sequentially paced at cycle lengths of 240 and 180 ms. Electrodes were placed in the superfusion chamber to record electrical activity throughout the studies and to monitor for pacing capture.

Average Ca^{2+} transients were computed from Rhod-2AM images using pixels from a small ROI having a diameter of 5 mm on the LV epicardium. Average transients were then analyzed using custom MATLAB (Mathworks) algorithms to measure the following parameters: duration from activation time to peak fluorescence (time-to-peak, TTP), duration from activation time to 30 % and 80 % relaxation (CaD30 and CaD80), and decay time constant (τ). The activation time was defined as the maximum of the second derivative, at the first detection of SR Ca^{2+} release. The return to baseline was fitted as a mono-exponential from 70 % height of the transient to the baseline to determine the decay time constant (τ) as described by Laurita et al. [26]. Average Ca^{2+} transient parameters were taken at 30 min after a perfusate switch to ensure the response had reached a steady-state.

We conducted parallel studies, as described above; with the exception that fNADH instead of Rhod-2AM was imaged. The objective was to determine if the inhibition of the actin-myosin ATPase with 4.75 μM of blebbistatin affected the dynamics of fNADH after administering DCA or pyruvate.

Measurement of SR calcium load

The effect of DCA and pyruvate on SR Ca^{2+} load was measured using neonatal myocyte monolayers and a caffeine surge protocol. Neonatal rat ventricular myocytes were isolated and plated from a heterogeneous population of hearts, as previously described [41, 42]. Intracellular Ca^{2+} transients were imaged using Fluo-4 and confocal fluorescence microscopy [42]. Cells were field stimulated at 0.2 Hz for 30 s (20 V, 10 ms BCL), followed by an injection of 20 mM caffeine to induce total SR calcium release [42]. The injection of caffeine was supplemented with 20 mM KCl and 1 mM verapamil to prevent rapid contractions. The average area under the curve (AUC) of three baseline transients was compared to the area of the large transient induced by the caffeine surge (AUC Ratio).

Arrhythmia scoring

Pressure and electrogram signals were examined to identify premature ventricular contractions (PVCs) and episodes of non-sustained ventricular tachycardia (NSVT). Arrhythmias were scored using a modified method from Jin et al. [20], where hearts having 20 or less PVCs received a score of 0 and hearts having more than 20 PVCs or one episode of NSVT for less than 2 s received a score of 1. We did not observe any heart to have NSVT longer than 2 s. We also did not observe VF or other significant arrhythmias, so scores beyond 1 were not necessary. All hearts received arrhythmia scores of either 0 or 1.

Statistics

Statistical analyses were performed in R. Data are presented as mean±standard error of mean. Significance was defined by $p<0.05$, unless noted as $p<0.01$. One-way ANOVAs with Tukey post hoc tests were used to identify significant differences between groups. A three-way ANOVA with Tukey post hoc tests were used to compare calcium transient

characteristics between baseline and treatments, pacing rates, and between treatments. All data were determined to be normal using the Shapiro–Wilk test.

Results

Control studies with identical KH solutions in each side of the dual perfusion apparatus confirmed that perfusate switching did not cause artifacts or alter heart function. Perfusate switching introduced a maximum temperature variation of less than ±1 °C and a heart rate change of less than 5 %. No other changes in heart function were detected. HR changes of less than 5 % were also measured when administering DCA or pyruvate.

LVDP and nNADH signals in all contracting heart studies consisted of three phases: a baseline phase (BP), a transient phase (TP), and a steady-state phase (SSP). The BP was the 10 min of baseline perfusion before a perfusate switch occurred. The TP was the period from the perfusate switch to when changes in LVDP or nNADH subsided. The SSP began when a given variable reached steady-state and corresponded to the time from the end of the TP to the end of study. Measurements did not maintain a stable steady state when pyruvate and lactate were included in the baseline perfusate so data were averaged 25 to 35 min post DCA administration (Post).

PDH activation by DCA and pyruvate

Pyruvate and DCA significantly increased PDH activity over baseline, with DCA demonstrating more pronounced activation (Fig. 1a). DCA activated PDH to the same level, with either 6 mM glucose or 6 mM glucose plus 1 mM lactate and 0.2 mM pyruvate included in the baseline perfusate (Fig. 1a, b).

Changes in left-ventricular developed pressure (LVDP)

Both 5 mM DCA and 5 mM pyruvate resulted in a transient reduction in LVDP. LVDP reached a minimum 1.6±0.4 min after perfusate was switched to 5 mM DCA (Fig. 2a and Table 1). LVDP then quickly increased, at which time PVCs began to appear (inset Fig. 2a). These PVCs consisted of a weakened contraction followed by a potentiated contraction. The steady-state LVDP with DCA was 47±6.5 % above base-line (Fig. 2d). In all but one DCA study, a significant number of PVCs and NSVT (<2-s duration) were observed throughout the TP and SSP. The number of hearts in each group with an arrhythmia score greater than one is listed in Table 2. A few additional studies were completed to determine if a higher dose of DCA would further reduce LVDP during the TP. In those studies 40 mM DCA was administered to hearts perfused with baseline perfusate containing 6 mM glucose. LVDP results were similar for 5 and 40 mM DCA, except that the transient minimum was more negative at 40 mM (−61.8±3.1 %) and time to steady-state was shorter (Table 1). The steady-state LVDP value was not different between the two DCA concentrations (57.8±11 %)

A similar pressure trend was observed in hearts that were switched to a perfusate including 5 mM pyruvate (Fig. 2b). The transient reduction in LVDP reached a minimum within 2.1±0.3 min. The transient LVDP minimum was significantly more depressed than that of 5 mM DCA (−44±0.89 vs. −26±4.0 %, $p<0.01$) (Fig. 2c). LVDP then quickly increased to a

steady-state level 88±5.3 % above baseline (Fig. 2b), a level significantly higher than that of 5 mM DCA ($p<0.01$). The time to steady-state was 22±0.2 min, significantly longer than that of 5 mM DCA ($p<0.05$) (Table 1). Average maximum and minimum LVDP derivatives (dP/dt) are plotted in Fig. 2e and f for each phase (BP, TP, and SSP) of DCA and pyruvate perfusion.

Arrhythmias with pyruvate were rare, with only one study having enough PVCs to result in an arrhythmia score of 1 during the TP (Table 2). Arrhythmias were not observed with pyruvate during the SSP of any study. Arrhythmias were also not observed when DCAwas administered with plasma levels of lactate and pyruvate. Likewise, arrhythmias were not observed with either DCA or pyruvate when blebbistatin was administered to image calcium transients.

The effects of 5 mM DCA on LVDP were different when baseline perfusate contained plasma levels of lactate and pyruvate (DCA-LP, Fig. 2c). A transient dip in LVDP was observed immediately after DCA administration, LVDP rose to 98±9 % above baseline after 30 min (Fig. 2c), and resulted in a significantly higher LVDP than when 5 mM DCAwas added with glucose as the sole exogenous fuel (Fig. 2d). Both contractility and lusitropy were significantly higher in the DCA-LP experiments compared to 5 mM DCA (Fig. 2e and f).

Changes in nNADH

Average NADH fluorescence peaked during the TP and then decreased to a sustained level in the SSP. nNADH signals and average data for each of the three phases are shown in Fig. 3a–c. When 5 mM pyruvate was administered, nNADH increased at a rate greater than that of DCA and peaked after 3.2±0.3 min (Table 1, Fig. 3b) at a level much higher than that of DCA (46.4±4.9 vs. 9.1±3.0 %, $p<0.05$). After the peak, nNADH gradually dropped, reaching a new stable level of 21±2.9 % at 17±0.2 min. Steady-state nNADH levels for pyruvate and DCA (with only 6 mM glucose as baseline exogenous fuel) were dramatically different (21.4±2.9 vs. −21.4±6.1 %, $p<0.01$), as shown in Fig. 3d. Similar results were obtained with 40 mM DCA (TP=10.6±3.5, SSP=−19.2±4.4) with no difference in average nNADH between the two DCA concentrations.

After administering 5 mM DCA with physiologic levels of lactate and pyruvate in the baseline perfusate, there was a period of increasing nNADH of varying rates that did not have a distinct steady-state phase (Fig. 3c). The inclusion of physiologic levels of lactate and pyruvate prevented the drop in nNADH below baseline in the TP that occurred when glucose was the only exogenous fuel (Fig. 3d). This result indicates that pyruvate production when glucose is the only exogenous fuel may limit NADH production after administering DCA.

The effect of actin-myosin ATPase inhibition on nNADH is shown in Fig. 4. The initial response for both DCA and pyruvate was a quick nNADH increase, similar to that observed in the contracting heart studies. However, a subsequent decrease of nNADH was not observed. nNADH plateaued at a higher steady-state level with pyruvate but continued to slowly increase throughout the duration of the study with DCA.

Cytosolic calcium kinetics

Cytosolic Ca^{2+} transients were measured from the anterior epicardial surface before and after administering DCA or pyruvate. Actin-myosin ATPase inhibition with blebbistatin was required to measure Ca^{2+} transients without motion artifact so Ca^{2+} measurements were carefully considered with respect to the nNADH results with blebbistatin shown in Fig. 4. Average Ca^{2+} transient kinetics were measured 30 min after a perfusate switch to ensure the absence of any transient response. This was longer than the time required to reach steady-state LVDP in the contracting heart experiments (Table 1).

Representative Ca^{2+} transients at the 240-ms pacing rate are shown in Fig. 5, with these signals reflecting the overall results shown in Fig. 6a-d. The significant effects of DCA or pyruvate on Ca^{2+} transient kinetics were to shorten CaD30 and TTP and lengthen τ. A narrower transient peak interval was observed with both DCA and pyruvate, observed as a shortened CaD30 (Fig. 6a), but the remaining Ca^{2+} uptake took longer (increased τ), ultimately resulting in a CaD80 that did not change compared to baseline.

Typical calcium transients from neonatal myocyte mono-layers superfused with baseline perfusate solution before and after a caffeine surge are shown in Fig. 7a. The ratio of the area under a transient after and before the caffeine surge was computed as the transient AUC ratio. Increased SR calcium load would be indicated as an increased transient AUC ratio compared to control. We observed that transient AUC ratios were significantly elevated after administering 5 mM DCA or pyruvate (Fig. 7b). Ratios were also higher for 5 mM pyruvate compared to 5 mM DCA (Fig.7b).

Discussion

Our systematic comparison of functional changes after the administration of DCA or exogenous pyruvate reveals that the responses of mitochondrial NADH and LVDP are biphasic and differ between the compounds. Both compounds activate PDH compared to baseline, though only DCA results in 100 % activation (Fig. 1b). In the presence of glucose alone, both compounds increase LVDP, but steady-state levels of NADH are higher than baseline with pyruvate while lower than baseline with DCA, consistent with reduced endogenous pyruvate. Indeed, DCA reduces circulating pyruvate concentration in patients [16] and reduces cytosolic pyruvate in isolated hearts provided with glucose and acetate as the only exogenous fuels [9]. Pyruvate stabilizes the RyR [52], so reduced cytosolic pyruvate likely increases the open probability of the RyR and may explain our finding of increased arrhythmias with DCA. Further supporting this, we have demonstrated that when DCA is administered in the presence of plasma concentrations of pyruvate and lactate, sustained NADH is higher than baseline and arrhythmia incidence is reduced. Taken together, we have shown in isolated perfused hearts, DCA increases LVDP in the normoxic myocardium in concert with a more oxidized mitochondrial redox state when exogenous lactate and pyruvate are not present. These results indicate the effects of DCA are dependent on circulating fuels available to the myocardium with a primary implication that DCA could create a condition of PDH substrate limitation subsequent to maximal PDH activation that increases arrhythmia susceptibility.

Left-ventricular developed pressure and contractility

LVDP transiently decreases then increases when either DCA or pyruvate is added to the perfusate, stabilizing at a level significantly higher than baseline without an increase in heart rate (Table 3). Increased LVDP with no change in heart rate after pyruvate administration is consistent with previous studies in normoxic hearts [10, 35]. The higher developed pressure is likely due to increased TCA cycle flux following PDH activation by pyruvate. Additionally, the mechanism of increased force production by pyruvate has been localized to the mitochondria, as blocking pyruvate from entering the mitochondrial matrix inhibits increased force [35]. Our results provide new data showing the time-course of LVDP changes after administering DCA. Furthermore, we show that steady-state LVDP with DCA is lower than that of exogenously administered pyruvate (Fig. 2d). While pyruvate and DCA both act to increase PDH flux [51], exogenous pyruvate provides ample PDH substrate, which supports higher LVDP. On the contrary, DCA would increase TCA cycle flux without activating the upstream producers of pyruvate (glycolytic enzymes), thereby causing a substrate limitation at PDH to limit further increases in LVDP.

Previous studies in isolated myocytes provide insight into the mechanism of the transient reduction of LVDP upon the administration of DCA and pyruvate [18, 46, 52]. Increased extracellular pyruvate increases the activity of the sarcolemmal H^+-monocarboxylate cotransporter [13, 40]. Co-transport of H^+ with pyruvate acidifies the cytosol, thereby reducing myofilament Ca^{2+} sensitivity and pressure development [18]. Jackson and Halestrap demonstrated that the up-take of DCA or pyruvate results in a pH reduction in liver cells, indicating that both compounds are likely co-transported into the cell with H^+ [19]. Our results in whole hearts are consistent with cytosolic acidification associated with the transport of DCA and pyruvate. Additionally, this phenomenon is concentration dependent, as 40 mM DCA results in a greater reduction in LVDP than 5 mM DCA. Our finding that 5 mM pyruvate or 5 mM DCA transiently reduce LVDP with a similar time course is consistent with the hypothesis that the sarcolemmal co-transporter is similar, or the same, for both compounds. We also found significant, but temporary, reductions in inotropy and lusitropy upon DCA and pyruvate administration, which are also consistent with cytosolic acidification (Fig. 2e-f). A previous study in cells indicates that cytosolic acidification is maintained [52], while other studies in cells and isolated muscle strips [18, 46] indicate that acidification is transient. Our results indicate that the acidification is likely transient in whole hearts.

Mitochondrial redox state

Our studies provide new data in normoxic myocardium for comparing changes in mitochondrial NADH after administering DCA or pyruvate. nNADH increases immediately upon administration of both compounds (Fig. 3a-c). This could be an intertwined result of increases in NADH production [12, 21] and lower NADH consumption due to the initially reduced LVDP in the TP. Maximum nNADH with 40 mM DCA was not significantly greater than that with 5 mM DCA, despite the transient reduction in LVDP being more significant. These results support the hypothesis that reduction in LVDP is due to cytosolic acidosis. The increase in nNADH is due not only to the decrease in LVDP, but increased metabolism as well. Subsequently, with both 5 and 40 mM DCA, nNADH begins to decline

as LVDP increases. The decline of nNADH is attributed to increased work output as reductions in LVDP are abolished. This interpretation is further supported by the absence of any decrease in nNADH when the actin-myosin ATPase is inhibited with blebbistatin (Fig. 4).

With pyruvate, nNADH stabilizes at a level substantially higher than baseline, consistent with previous studies [3, 43]. This is also consistent with lower FAD^+, as observed by Zima et al. after the introduction of pyruvate to individual ventricular myocytes [52]. Others have shown that increased pyruvate oxidation increases cytosolic phosphorylation potential during normoxia and post-ischemic recovery [10], to which increased LVDP and contractility have been attributed [44]. Although we did not measure $[ATP]/[ADP][P_i]$, cytosolic phosphorylation potential can be inferred from changes in mitochondrial NADH when glucose-only perfusate is supplemented with pyruvate [43]. Altogether, our SSP results are consistent with previous observations of higher cytosolic phosphorylation potential in hearts perfused with pyruvate [10, 11, 35].

Our hypothesis that the administration of DCA to a normoxic heart would lower mitochondrial steady-state NADH when glucose is the only exogenous supplied fuel is supported by the reduction of NADH to a level lower than baseline (Fig. 3d). Since DCA terminates regulation of PDH via negative feedback loops, leaving PDH in an active state despite low levels of pyruvate [48], we surmise that DCA depletes endogenous pyruvate if only glucose is available. Indeed, it has been shown DCA reduces cytosolic pyruvate in the heart [9]. After administering DCA with only glucose, the only available source of pyruvate is that of which is glycolytically produced, on the order of 67 μM [35]. Furthermore, increased workload increases NADH consumption rate and decreases mitochondrial NADH [3, 4, 8]. Our results showing DCA simultaneously increases LVDP and decreases nNADH are consistent with the concept that in the absence of abundant substrate increased work output is associated with a decrease in steady-state mitochondrial NADH.

Cytosolic calcium transient kinetics

We show for the first time the effect of DCA and pyruvate on the kinetics of cytosolic calcium transients in isolated perfused hearts. With both compounds, we found reductions in Ca^{2+} TTP and CaD30. We also found that CaD80 remained unchanged: a combined effect of shortened CaD30 with lengthening of τ. These results are consistent with increased SR Ca^{2+} load as a result of increased cytosolic phosphorylation potential [33]. Indeed, studies in isolated cardiac myocytes found that pyruvate increases SR Ca^{2+} load [18, 52] due to increased cytosolic phosphorylation potential, which result in increased Ca^{2+} transient amplitude [46, 52] and increased systolic contractile force [35, 52]. Although nNADH dropped below baseline in contracting hearts with DCA (Fig. 3a), nNADH rose steadily above baseline with DCA when the conditions of the calcium measurements were reproduced by inhibiting the actin-myosin ATPase with blebbistatin (Fig. 4). This result supports the evidence that elevated cytosolic phosphorylation potential with both DCA and pyruvate was the primary mechanism of the observed changes in Ca^{2+} kinetics.

Our finding of reduced TTP corresponds to increased RyR synchronization, despite a possible reduction in RyR open probability by the presence of pyruvate [52]. Higher

cytosolic phosphorylation potential should enable the SERCA pump to maintain higher trans-SR Ca^{2+} gradients. However, longer τ indicates that SERCA requires more time to re-sequester the larger amount of Ca^{2+} released, particularly in the later part of the Ca^{2+} uptake phase. This interpretation is aligned with results of Torres et al. that show increases in relaxation time in trabeculae muscle after administering pyruvate [46]. Our finding of reductions in CaD30 is evidence that SERCA activity is increased in the early portion of the calcium transient. This would also explain the narrowing of the transient peak observed with DCA and pyruvate in Fig. 5b, c. DCA caused more significant shortening of CaD30 than pyruvate (Fig. 6a). This may reflect that more Ca^{2+} is released from the SR with pyruvate, as demonstrated by our myocyte SR load experiments which show pyruvate causes more significant elevation of SR load than DCA (Fig. 7b). With DCA and pyruvate, the measured reductions of TTP are approximately 2 ms, but CaD30 reductions are approximately 5–10 ms, indicating that the changes in CaD30 are not solely due to changes in TTP and are likely the result of improved uptake by SERCA and/or extrusion by the Na^{+}/Ca^{2+} transporter. However, the absence of a change in CaD80 indicates this increased uptake rate was not maintained throughout the Ca^{2+} transient.

To our knowledge the only study that measured myocardial Ca^{2+} content before and after DCA found that total myocardial Ca^{2+} was unchanged [1]. Our results indicate DCA does indeed increase SR calcium load in isolated myocytes (Fig. 7b). However, this may only be the case when work is low (electromechanically uncoupled hearts and isolated myocytes) or when there is additional substrate (circulating lactate at 1 mM and pyruvate at 0.2 mM). Greater LVDP and inotropy with DCA in the contracting heart experiments is evidence of increased actin-myosin ATPase activity, which predicts increased Ca^{2+} transient amplitude. Deeper insight will require additional studies that will likely involve measuring cytosolic Ca^{2+} transient amplitudes and SR Ca^{2+} load in contracting hearts before and after administering DCA.

Conclusion

There is consensus that DCA improves post-ischemic cardiac recovery in isolated perfused hearts, but mechanisms by which DCA improves function in normoxic myocardium are not completely understood. We show that although DCA and pyruvate activate PDH at different levels they increase steady-state contractility and similarly alter calcium kinetics and increase SR load. Steady-state levels of mitochondrial NADH are different between DCA and pyruvate and depend upon the availability of exogenous fuels. When PDH is maximally activated with DCA, the response in normoxic myocardium, when glucose is the only exogenous fuel, is an increase in LVDP and contractility, a drop in mitochondrial NADH, and elevated incidence of premature ventricular contractions. Plasma levels of lactate and pyruvate mitigate the drop in mitochondrial NADH and prevent premature ventricular contractions.

Limitations

Study limitations include the typical shortcomings of ex vivo-perfused heart preparations: perfusion with a crystalloid perfusate instead of blood, the non-physiologic working

condition of isovolumic contraction, and the use of an electrome-chanical uncoupling agent for the Ca^{2+} imaging studies [24]. NADH fluorescence signals could be contaminated by changes in myoglobin absorbance and changes in cell density; however, such contamination is unlikely because none of our experimental perturbations induced ischemia or hypoxia. Our nNADH measurements could also be contaminated by the antioxidant effect of pyruvate [5] as well as possible contamination of NADPH fluorescence from the cytosol, although this is unlikely due significant enhancement of mitochondrial NADH by the binding of NADH to Complex I [7].

Acknowledgments

We acknowledge Dr. Jay H. Kramer and Dr. Brian Glancy for helpful discussions for determining PDH activity and Nate Serafino for technical assistance. This study was supported by NIH grant HL095828 (to MWK), NIH grant K99ES023477 (to NGP), and American Heart Association Postdoctoral Fellowship 14POST20490181 (to SKG).

References

1. Aasum E, Steigen T, Larsen T. Stimulation of carbohydrate metabolism reduces hypothermia-induced calcium load in fatty acid-perfused rat hearts. J Mol Cell. 1997; 534:527–534.
2. Asfour H, Wengrowski AM, Jaimes R 3rd, Swift LM, Kay MW. NADH fluorescence imaging of isolated biventricular working rabbit hearts. J Vis Exp. 2012; 65:1–7.
3. Ashruf JF, Coremans JM, Bruining HA, Ince C. Increase of cardiac work is associated with decrease of mitochondrial NADH. Am J Physiol. 1995; 269:H856–H862. [PubMed: 7573528]
4. Ashruf JF, Coremans JM, Bruining HA, Ince C. Mitochondrial NADH in the Langendorff rat heart decreases in response to increases in work: increase of cardiac work is associated with decrease of mitochondrial NADH. Adv Exp Med Biol. 1996; 388:275–282. [PubMed: 8798823]
5. Bassenge E, Sommer O, Schwemmer M, Bünger R. Antioxidant pyruvate inhibits cardiac formation of reactive oxygen species through changes in redox state. Am J Physiol Heart Circ Physiol. 2000; 279:H2431–H2438. [PubMed: 11045981]
6. Bersin RM, Stacpoole PW. Dichloroacetate as metabolic therapy for myocardial ischemia and failure. Am Hear J. 1997; 134:841–855.
7. Blinova K, Levine RL, Boja ES, Griffiths GL, Shi Z-D, Ruddy B, Balaban RS. Mitochondrial NADH fluorescence is enhanced by complex I binding. Biochemistry. 2008; 47:9636–9645. [PubMed: 18702505]
8. Brandes R, Bers DM. Increased work in cardiac trabeculae causes decreased mitochondrial NADH fluorescence followed by slow recovery. Biophys J. 1996; 71:1024–1035. [PubMed: 8842239]
9. Bünger R, Mallet RT. Mitochondrial pyruvate transport in working guinea-pig heart. Work-related vs. carrier-mediated control of pyruvate oxidation. Biochim Biophys Acta Biomembr. 1993; 1151:223–236.
10. Bünger R, Mallet RT, Hartman DA. Pyruvate-enhanced phosphorylation potential and inotropism in normoxic and postischemic isolated working heart. Near-complete prevention of reperfusion contractile failure. Eur J Biochem. 1989; 180:221–233. [PubMed: 2707262]
11. Chen W, London R, Murphy E, Steenbergen C. Regulation of the Ca2+ gradient across the sarcoplasmic reticulum in perfused rabbit heart. A 19F nuclear magnetic resonance study. Circ Res. 1998; 83:898–907. [PubMed: 9797338]
12. Combs C, Balaban RS. Direct imaging of dehydrogenase activity within living cells using enzyme-dependent fluorescence recovery after photobleaching (ED-FRAP). Biophys J. 2001; 80:2018–2028. a. [PubMed: 11259315]
13. De Hemptinne A, Marrannes R, Vanheel B. Influence of organic acids on intracellular pH. Am J Physiol Cell Physiol. 1983; 245:C178–C183.

14. Fedorov VV, Lozinsky IT, Sosunov EA, Anyukhovsky EP, Rosen MR, Balke CW, Efimov IR. Application of blebbistatin as an excitation-contraction uncoupler for electrophysiologic study of rat and rabbit hearts. Heart Rhythm. 2007; 4:619–626. [PubMed: 17467631]
15. Gohil K, Jones DA. A sensitive spectrophotometric assay for pyruvate dehydrogenase and oxoglutarate dehydrogenase complexes. Biosci Rep. 1983; 3:1–9. [PubMed: 6839008]
16. Gore DC, Jahoor F, Hibbert JM, DeMaria EJ. Lactic acidosis during sepsis is related to increased pyruvate production. Not deficits in tissue oxygen availability. Ann Surg. 1996; 224:97–102. [PubMed: 8678625]
17. Gottlieb R, Magnus R. Digitalis und Herzabeit. Nach Versuchen an uberlebenden Warmbluterherzen. Path Pharamakol. 1904; 51:30–63.
18. Hasenfuss G, Maier LS, Hermann H-P, Lüers C, Hünlich M, Zeitz O, Janssen PML, Pieske B. Influence of pyruvate on contractile performance and Ca^{2+} cycling in isolated failing human myocardium. Circulation. 2002; 105:194–199. [PubMed: 11790700]
19. Jackson VN, Halestrap AP. The kinetics, substrate, and inhibitor specificity of the monocarboxylate (lactate) transporter of rat liver cells determined using the fluorescent intracellular pH indicator, 2′,7′-bis(carboxyethyl)-5(6)-carboxyfluorescein. J Biol Chem. 1996; 271:861–868. [PubMed: 8557697]
20. Jin H, Nass RD, Joudrey PJ, Lyon AR, Chemaly ER, Rapti K, Akar FG. Altered spatiotemporal dynamics of the mitochondrial membrane potential in the hypertrophied heart. Biophys J. 2010; 98:2063–2071. [PubMed: 20483313]
21. Joubert F, Fales HM, Wen H, Combs CA, Balaban RS. NADH enzyme-dependent fluorescence recovery after photobleaching (ED-FRAP): applications to enzyme and mitochondrial reaction kinetics, in vitro. Biophys J. 2004; 86:629–645. [PubMed: 14695307]
22. Kang YH, Mallet RT, Bünger R. Coronary autoregulation and purine release in normoxic heart at various cytoplasmic phosphorylation potentials: disparate effects of adenosine. Pflugers Arch. 1992; 421:188–199. [PubMed: 1528716]
23. Kobayashi K, Neely JR. Effects of ischemia and reperfusion on pyruvate dehydrogenase activity in isolated rat hearts. J Mol Cell Cardiol. 1983; 15:359–367. [PubMed: 6876185]
24. Kuzmiak-Glancy S, Jaimes R, Wengrowski AM, Kay MW. Oxygen demand of perfused heart preparations: how electromechanical function and inadequate oxygenation affect physiology and optical measurements. Exp Physiol. 2015 doi: 10.1113/EP085042.
25. Laughlin MR, Taylor J, Chesnick AS, DeGroot M, Balaban RS. Pyruvate and lactate metabolism in the in vivo dog heart. Am J Physiol. 1993; 264:H2068–H2079. [PubMed: 8322935]
26. Laurita KR, Katra R, Wible B, Wan X, Koo MH. Transmural heterogeneity of calcium handling in canine. Circ Res. 2003; 92:668–675. [PubMed: 12600876]
27. Lewandowski ED, Johnston DL. Reduced substrate oxidation in postischemic myocardium: 13C and 31P NMR analyses. Am J Physiol Hear Circ Physiol. 1990; 258:H1357–H1365.
28. Lewandowski ED, White LT. Pyruvate dehydrogenase influences postischemic heart function. Circulation. 1995; 91:2071–2079. [PubMed: 7895366]
29. Liedtke AJ. Alterations of carbohydrate and lipid metabolism in the acutely ischemic heart. Prog Cardiovasc Dis. 1981; 23:321–336. [PubMed: 7012926]
30. Liu B, Clanachan AS, Schulz R, Lopaschuk GD. Cardiac efficiency is improved after ischemia by altering both the source and fate of protons. Circ Res. 1996; 79:940–948. [PubMed: 8888686]
31. Lloyd S, Brocks C, Chatham JC. Differential modulation of glucose, lactate, and pyruvate oxidation by insulin and dichloroacetate in the rat heart. Am J Physiol Heart Circ Physiol. 2003; 285:H163–H172. [PubMed: 12793977]
32. Lopaschuk GD, Wambolt RB, Barr RL. An imbalance between glycolysis and glucose oxidation is a possible explanation for the detrimental effects of high levels of fatty acids during aerobic reperfusion of ischemic hearts. J Pharmacol Exp Ther. 1993; 264:135–144. [PubMed: 8380856]
33. Mallet RT, Bunger R. Energetic modulation of cardiac inotropism and sarcoplasmic. Biochim Biophys Acta.
34. Mallet R, Hartman D, Bunger R. Glucose requirement for postischemic recovery of perfused working heart. Eur J Biochem. 1990; 188:481–493. [PubMed: 2318214]

35. Mallet RT, Sun J. Mitochondrial metabolism of pyruvate is required for its enhancement of cardiac function and energetics. Cardiovasc Res. 1999; 42:149–161. [PubMed: 10435006]
36. Masoud WGT, Ussher JR, Wang W, Jaswal JS, Wagg CS, Dyck JR, Lygate CA, Neubauer S, Clanachan AS, Lopaschuk GD. Failing mouse hearts utilize energy inefficiently and benefit from improved coupling of glycolysis and glucose oxidation. Cardiovasc Res. 2014; 101:30–38. [PubMed: 24048945]
37. McVeigh JJ, Lopaschuk GD. Dichloroacetate stimulation of glucose oxidation improves recovery of ischemic rat hearts. Am J Physiol. 1990; 259:H1079–H1085. [PubMed: 2221115]
38. Nasa Y, Ichihara K, Abiko Y. Myocardial non-esterified fatty acids during normoxia and ischemia in Langendorff and working rat hearts. Jpn J Pharmacol. 1990; 53:129–133. [PubMed: 2112658]
39. Patel TB, Olson MS. Regulation of pyruvate dehydrogenase complex in ischemic rat heart. Am J Physiol. 1984; 246:H858–H864. [PubMed: 6742152]
40. Poole RC, Halestrap AP. Transport of lactate and other monocarboxylates across mammalian plasma membranes. Am J Physiol. 1993; 264:C761–C782. [PubMed: 8476015]
41. Posnack NG, Brooks D, Chandra A, Jaimes R 3rd, Sarvazyan N, Kay MW. Physiological response of cardiac tissue to Bisphenol A: alterations in ventricular pressure and contractility. Am J Physiol Heart Circ Physiol. doi: 10.1152/ajpheart.00272.2015.
42. Posnack NG, Idrees R, Ding H, Jaimes R 3rd, Stybayeva G, Karabekian Z, Laflamme MA, Sarvazyan N. Exposure to phthalates affects calcium handling and intercellular connectivity of human stem cell-derived cardiomyocytes. PLoS One. 2015; 10:e0121927. [PubMed: 25799571]
43. Scholz TD, Laughlin MR, Balaban RS, Kupriyanov VV, Heineman FW. Effect of substrate on mitochondrial NADH, cytosolic redox state, and phosphorylated compounds in isolated hearts. Am J Physiol. 1995; 268:H82–H91. [PubMed: 7840306]
44. Schulze K, Duschek C, Lasley RD, Bünger R. Adenosine enhances cytosolic phosphorylation potential and ventricular contractility in stunned guinea pig heart: receptor-mediated and metabolic protection. J Appl Physiol. 2007; 102:1202–1213. [PubMed: 17341737]
45. Taniguchi M, Wilson C, Hunter CA, Pehowich DJ, Clanachan AS, Lopaschuk GD. Dichloroacetate improves cardiac efficiency after ischemia independent of changes in mitochondrial proton leak. Am J Physiol Heart Circ Physiol. 2001; 280:H1762–H1769. [PubMed: 11247790]
46. Torres CAA, Varian KD, Canan CH, Davis JP, Janssen PML. The positive inotropic effect of pyruvate involves an increase in myofilament calcium sensitivity. PLoS One. 2013; 8:e63608. [PubMed: 23691074]
47. Vincent G, Khairallah M, Bouchard B, Des RC. Metabolic phenotyping of the diseased rat heart using 13C-substrates and ex vivo perfusion in the working mode. Mol Cell Biochem. 2003; 242:89–99. [PubMed: 12619870]
48. Wahr JA, Olszanski D, Childs KF, Bolling SF. Dichloroacetate enhanced myocardial functional recovery post-ischemia: ATP and NADH recovery. J Surg Res. 1996; 63:220–224. [PubMed: 8661201]
49. Wengrowski AM, Kuzmiak-Glancy S, Jaimes R 3rd, Kay MW. NADH changes during hypoxia, ischemia, and increased work differ between isolated heart preparations. Am J Physiol Heart Circ Physiol. 2014; 306:H529–H537. [PubMed: 24337462]
50. White LT, O'Donnell JM, Griffin J, Lewandowski ED. Cytosolic redox state mediates postischemic response to pyruvate dehydrogenase stimulation. Am J Physiol. 1999; 277:H626–H634. [PubMed: 10444488]
51. Whitehouse S, Cooper RH, Randle PJ. Mechanism of activation of pyruvate dehydrogenase by dichloroacetate and other halogenated carboxylic acids. Biochem J. 1974; 141:761–774. [PubMed: 4478069]
52. Zima AV, Kockskämper J, Mejia-Alvarez R, Blatter LA. Pyruvate modulates cardiac sarcoplasmic reticulum Ca^{2+} release in rats via mitochondria-dependent and -independent mechanisms. J Physiol. 2003; 550:765–783. [PubMed: 12824454]

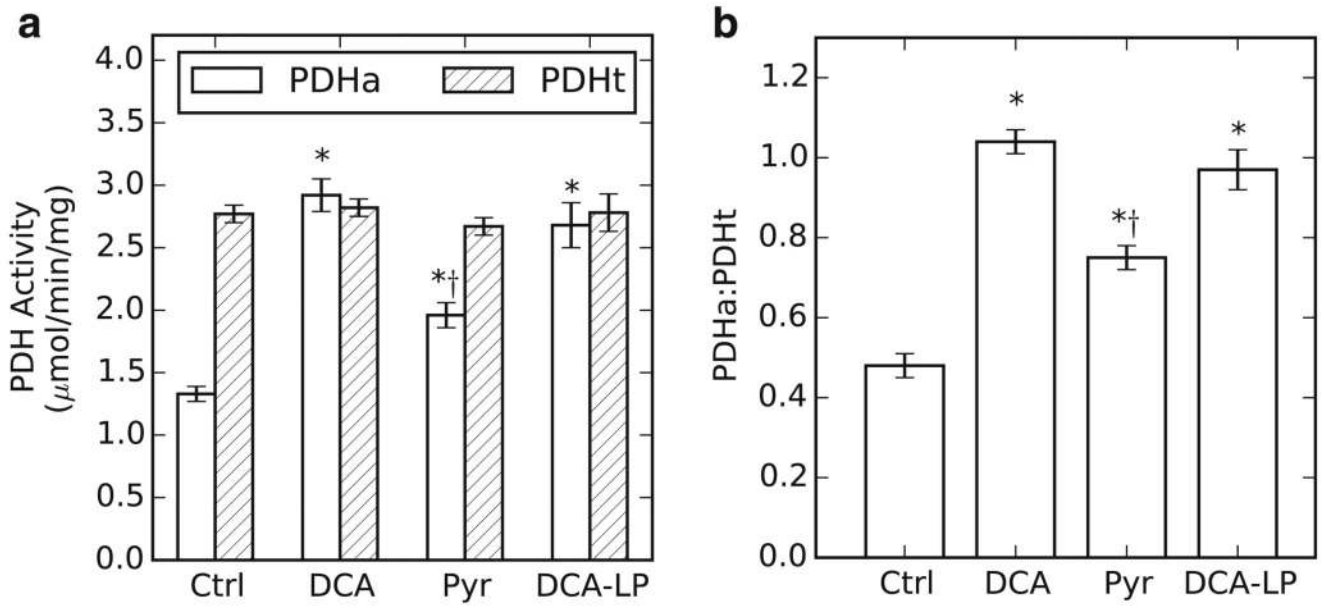

Fig. 1.

(**a**) Measured active PDH (*PDHa*) and total PDH (*PDHt*) activities from hearts perfused with 6 mM glucose (*Ctrl*), 6 mM glucose+5 mM DCA (*DCA*), 6 mM glucose+5 mM pyruvate (*Pyr*), and 6 mM glucose+1 mM lactate+0.2 mM pyruvate+5 mM DCA (*DCA-LP*). (**b**) Ratios of PDHa:PDHt. *n*=3 per group. *Asterisk*, significantly different than control. *Dagger*, significantly different than 5 mM DCA

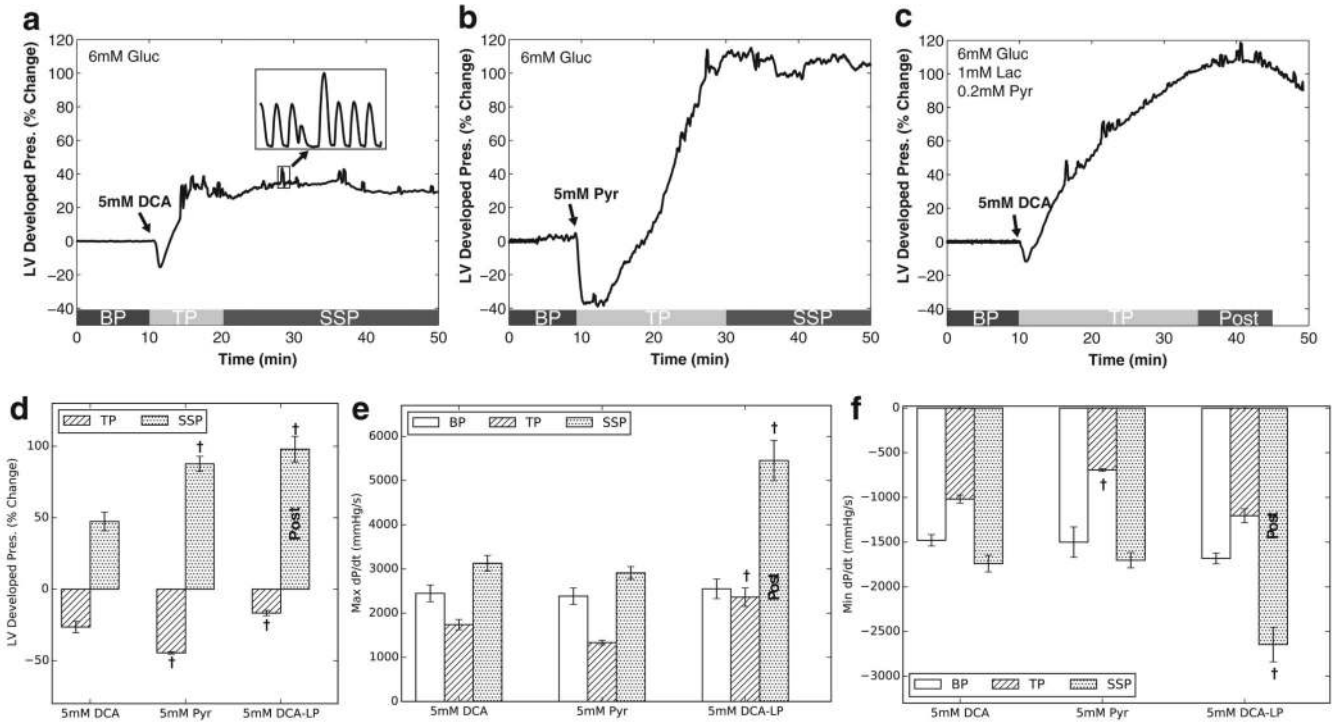

Fig. 2.

Changes from baseline in left-ventricular developed pressure (*LVDP*) upon the administration of DCA or pyruvate. Representative LVDP signals upon the administration of (**a**) 5 mM DCA or (**b**) 5 mM pyruvate at 10 min. Normalized LVDP is shown during the baseline phase (*BP*), transient phase (*TP*), and steady-state phase (*SSP*). When (**c**) 5 mM DCA was administered in the presence of 1 mM lactate and 0.2 mM pyruvate, there was no distinct steady-state phase. The trough value was used for TP and the average LVDP between 25 and 35 min after administration (*Post*) was compared to SSP. Average LVDP data (**d**), max dP/dt (**e**), and min dP/dt (**f**) during TP and SSP (or *Post*) for each group. *n*=3–5 per group. *Dagger*, significantly different than 5 mM DCA

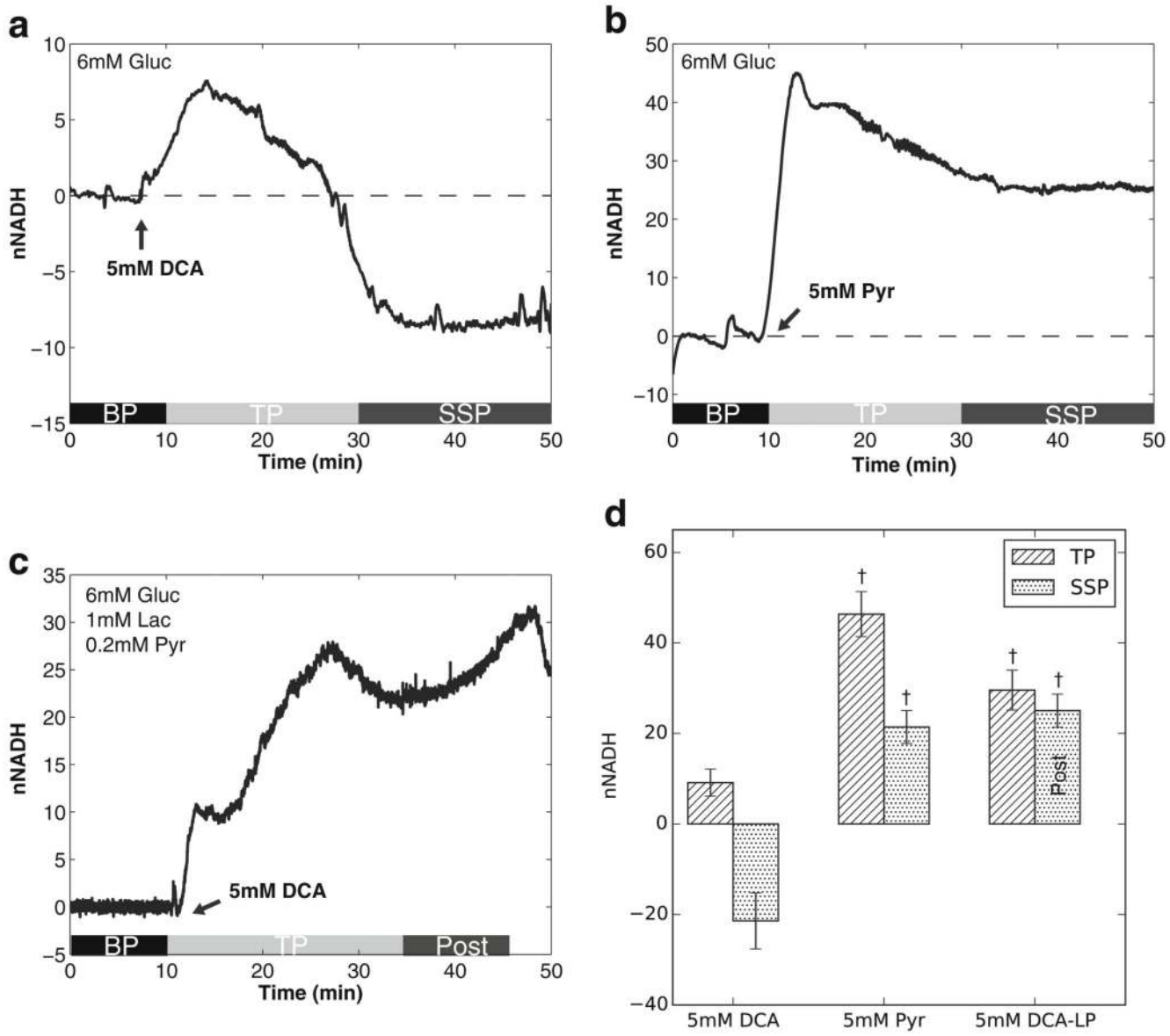

Fig. 3.

Changes from baseline in fNADH after administering DCA or pyruvate. Representative normalized fNADH (*nNADH*) from the epicardium of isovolumic contracting hearts upon the administration of (**a**) 5 mM DCA, (**b**) 5 mM pyruvate, and (**c**) 5 mM DCA in the presence of 1 mM lactate and 0.2 mM pyruvate. Fluorescence was normalized as described in the Methods. (**d**) Average nNADH during TP and SSP (or *Post*) for each group. *n*=3–5 per group. *Dagger*, significantly different than 5 mM DCA

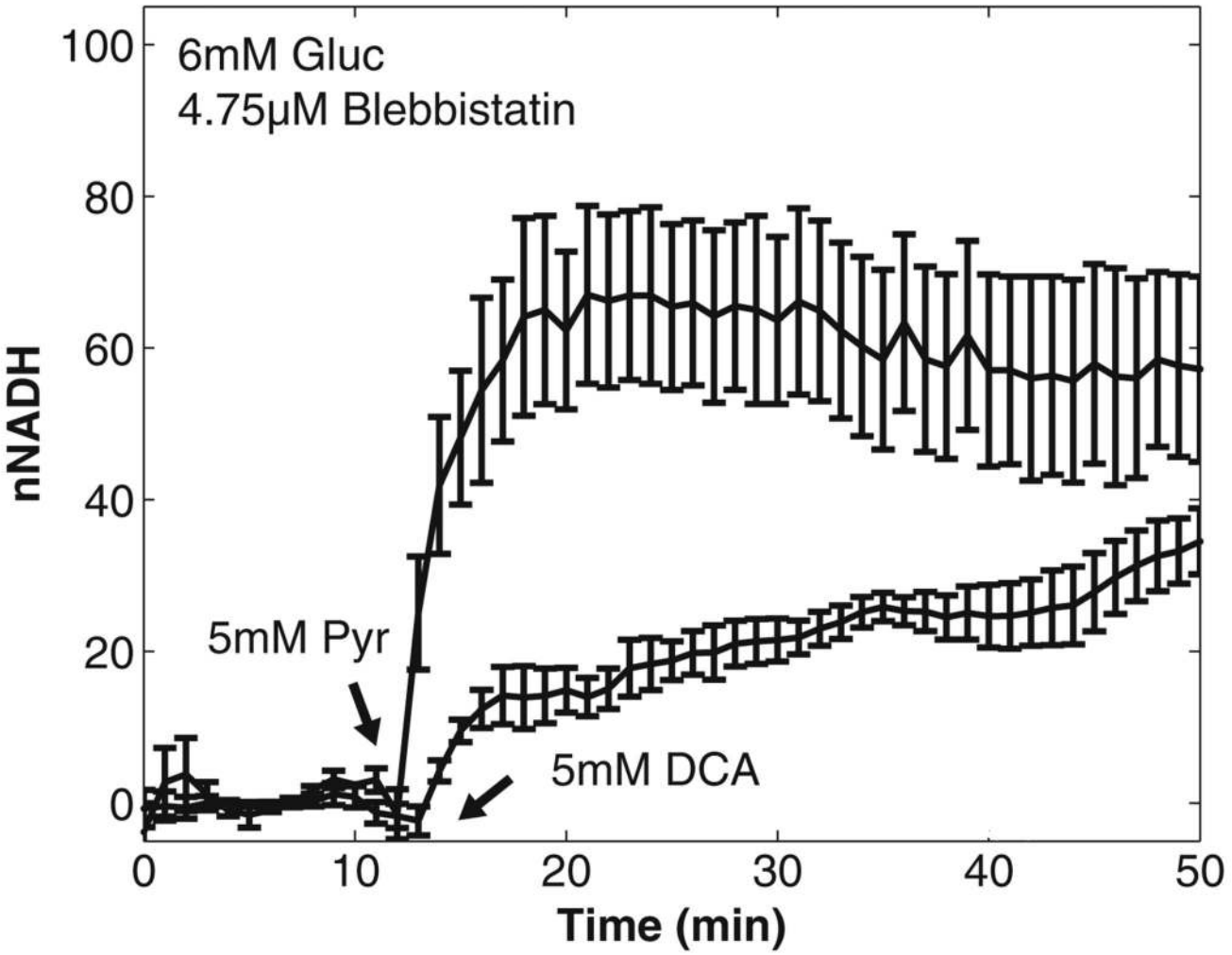

Fig. 4.

Changes in epicardial NADH fluorescence after administering DCA or pyruvate in hearts electromechanically uncoupled with blebbistatin.

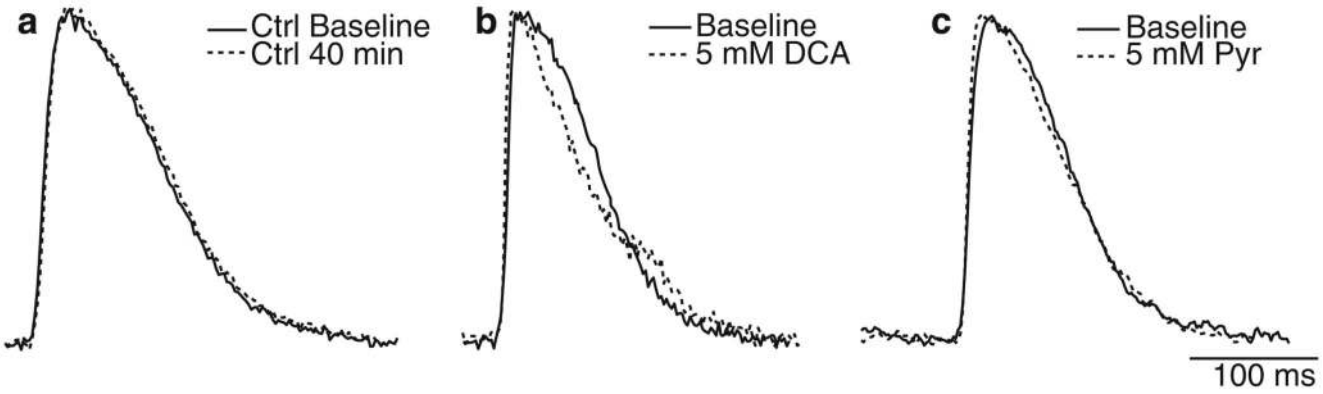

Fig. 5.

Representative, normalized calcium transients. Transients were acquired during pacing at 240-ms-cycle length after 10 min of baseline (with 6 mM glucose) and either (**a**) 30 additional min of control, (**b**) 30 min of 5 mM DCA administration, or (**c**) 30 min of 5 mM pyruvate administration

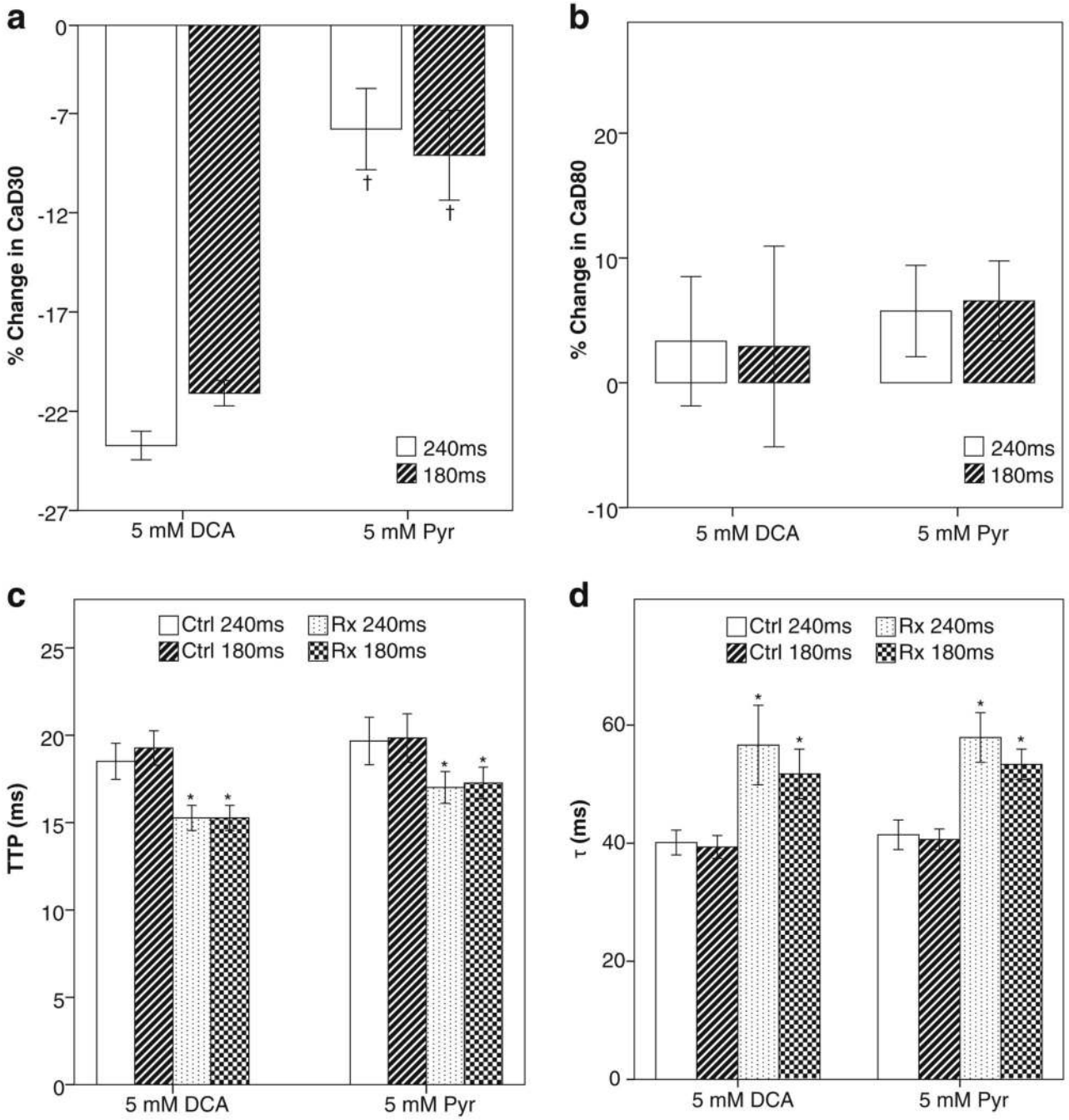

Fig. 6.

Changes in Ca^{2+} transient kinetics after administering DCA or pyruvate. Percent change in Ca^{2+} transient duration at (**a**) 30 % recovery (*CaD30*) and (**b**) 80 % recovery (*CaD80*). *Dagger*, significantly different than 5 mM DCA. Change in (**c**) time-to-peak (*TTP*) and (**d**) decay time constant (τ). *Asterisk*, treatment (*Rx*) significantly different than control. *n*=5 per group

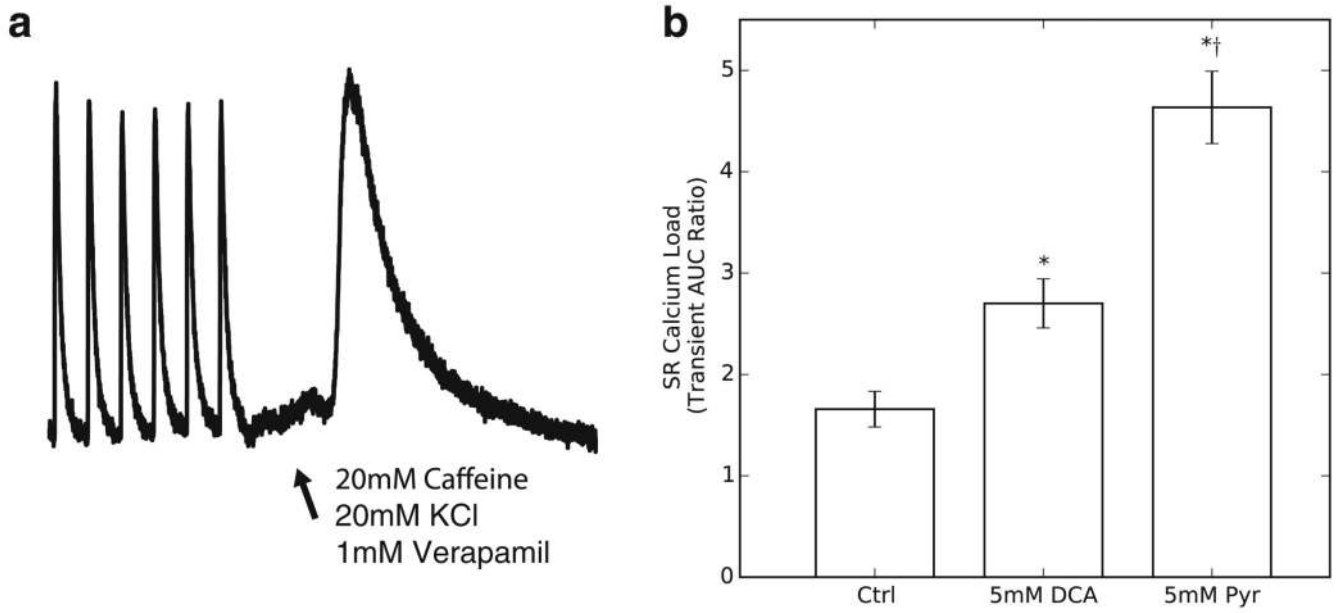

Fig. 7.

Measurements of SR calcium load by caffeine. (**a**) Representative calcium transients during SR load experiments. (**b**) The ratio of area under the curve of the caffeine induced calcium transient to the area under the curve of three averaged baseline transients in each group. *n*=3 per group. *Asterisk*, significantly different than control. *Dagger*, significantly different than 5 mM DCA

Table 1

Time to peak/trough and time to steady-state of LVDP and a NADH after administering DCA or pyruvate

		5 mM DCA	5 mM Pyruvate	40 mM DCA
LVDP	Time-to-trough	1.6±0.4	2.1±0.3	1.5±0.2
	Time-to-SS	11±1.2	22±0.2[a]	5.9±0.5[a]
NADH	Time-to-peak	2.1±0.6	3.2±0.3[b]	2.2±0.4
	Time-to-SS	9.6±0.9	17±0.2 [ba]	5.5±0.8[a]

Time (in minutes) for NADH and LVDP signals to achieve peak (NADH) or trough (LVDP) as well as the time to achieve new steady-state after administering DCA or pyruvate. Data represents mean±SE. *n*=3-5 per group

[a] Significantly different than corresponding 5 mM DCA value

[b] Significantly different from 5 mM pyruvate LVDP

Table 2

Arrhythmia scores

		Transient phase	Steady-state phase
Contracting	5 mM DCA	4/5	4/5
	5 mM pyruvate	1/3	0/3
	40 mM DCA	3/3	3/3
	5 mM DCA-LP	0/4	1/4 (Post)
Non-contracting (Blebbistatin)	5 mM DCA	0/4	N/A
	5 mM pyruvate	0/4	0/4

Number of hearts within each group that experienced arrhythmias during the transient or steady-state phases. See Materials and methods for arrhythmia scoring criteria

Table 3

Summary of functional, metabolic, and calcium cycling differences between 5 mM DCA and 5 mM pyruvate during steady-state

	DCA vs. baseline	Pyruvate vs. baseline	DCA vs. pyruvate
PDHa:PDHt	Greater *	Greater *	Greater *
Heart rate	ND	ND	ND
LVDP	Greater *	Greater *	Lower *
Max dP/dt	Greater *	Greater (ns)	ND
Min dP/dt	Lower *	Lower (ns)	ND
LVDP TP Dur	NA	NA	Shorter *
NADH TP Dur	NA	NA	Shorter *
nNADH	Lower *	Greater *	Lower *
CaD30	Shorter *	Shorter *	ND
CaD80	ND	ND	ND
CaT TTP	Shorter *	Shorter *	ND
CaT τ	Longer *	Longer *	ND

ND no difference, *NA* not available

* $p<0.05$